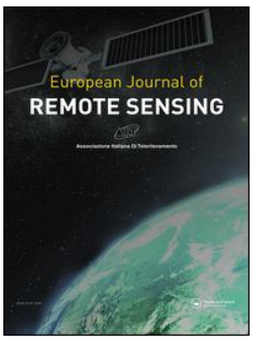

European Journal of Remote Sensing

ISSN: (Print) 2279-7254 (Online) Journal homepage: http://www.tandfonline.com/loi/tejr20

Single-tree detection in high-density LiDAR data from UAV-based survey

M. Balsi, S. Esposito, P. Fallavollita & C. Nardinocchi

To cite this article: M. Balsi, S. Esposito, P. Fallavollita & C. Nardinocchi (2018) Single-tree detection in high-density LiDAR data from UAV-based survey, European Journal of Remote Sensing, 51:1, 679-692, DOI: 10.1080/22797254.2018.1474722

To link to this article: https://doi.org/10.1080/22797254.2018.1474722

Published online: 12 Jun 2018.

EUROPEAN JOURNAL OF REMOTE SENSING, 2018
VOL. 51, NO. 1, 679–692
https://doi.org/10.1080/22797254.2018.1474722

Taylor & Francis
Taylor & Francis Group

Single-tree detection in high-density LiDAR data from UAV-based survey

M. Balsi [a], S. Esposito[b], P. Fallavollita[a,b] and C. Nardinocchi [c]

[a]DIET, Department of Information Engineering, Electronics and Communications, Sapienza University of Rome, Italy; [b]Oben s.r.l., Sassari, Italy; [c]DICEA, Department of Civil, Constructional and Environmental Engineering, Sapienza University of Rome, Italy

ABSTRACT

Unmanned aerial vehicle-based LiDAR survey provides very-high-density point clouds, which involve very rich information about forest detailed structure, allowing for detection of individual trees, as well as demanding high computational load. Single-tree detection is of great interest for forest management and ecology purposes, and the task is relatively well solved for forests made of single or largely dominant species, and trees having a very evident pointed shape in the upper part of the canopy (in particular conifers). Most authors proposed methods based totally or partially on search of local maxima in the canopy, which has poor performance for species that have flat or irregular upper canopy, and for mixed forests, especially where taller trees hide smaller ones. Such considerations apply in particular to Mediterranean hardwood forests. In such context, it is imperative to use the whole volume of the point cloud, however keeping computational load tractable. The authors propose the use of a methodology based on modelling the 3D-shape of the tree, which improves performance with respect to maxima-based models. A case study, performed on a hazel grove, is provided to document performance improvement on a relatively simple, but significant, case.

ARTICLE HISTORY
Received 3 July 2017
Revised 2 May 2018
Accepted 6 May 2018

KEYWORDS
Airborne laser scanning (ALS); forestry; Unmanned aerial vehicle (UAV); trees

Introduction

Sustainable forests management (SFM) is emerging as an increasingly important activity both for economic and environmental purposes. In fact, forests not only provide timber resources, but also act as carbon sinks and biodiversity safeguards.

SFM requires detailed information about the forest composition and biomass content. To this purpose, individual tree mapping and characterization is instrumental to several SFM activities. Traditional methods for detailed ground-based forest inventory are too expensive and time-consuming to be applied on large scale; therefore, a strong need for automatization of individual tree detection (ITD) has emerged.

Availability of airborne LiDAR scanners, with increasing performance and lowering cost, makes such kind of remote sensing particularly useful for the purpose of ITD. While point density has been limited until recently to under 10 points/m^2, low-altitude scanning by means of unmanned aerial vehicles (UAV) has now made one-order-of-magnitude-larger densities practical, even though on smaller areas (e.g. Sačkov, Bucha, Santopuoli, Lasserre, & Marchetti, 2016 – *other self-citation to be added after blind review*). Quite high densities can however also be obtained using small helicopters. The large amount of data thus gathered makes the need for automatized processing even stronger.

The first and most popular approach used is based on generating a Canopy Height Model (CHM) in raster form, and searching for local maxima in the top of the canopy, indicating position of a tree (Kaartinen and Hyppä, 2008). Delineation of the area occupied by a tree was subsequently performed by region growing, typically watershed, using the maxima as seeds. Such approach was at the basis of most methods applied by participants to the EuroSDR contest held in 2008 (Kaartinen & Hyppä, 2008), that set a state-of-the-art milestone for single tree detection about one decade ago, and Kaartinen et al. (2012) published a comparison of the methods and results adding to the set a method based on a simple Laplacian filter for local maxima detection (LOCM) after smoothing as well as a multiscale Laplacian of Gaussian (LOG). Jakubowski, Li, Guo, and Kelly (2013) reviewed methods proposed to date, comparing with their own, also based on finding local maxima and valleys of the CHM (Li, Guo, Jakubowski, & Kelly, 2012). Liu, Im, and Quackenbush (2015) proposed a method to improve tree segmentation resulting from watershed methods, by applying an original algorithm that iteratively adjusts crown boundaries (in a fashion similar to active contours techniques) to correspond more closely to actual tree shape, also allowing for topological transformations. However, this method requires collecting training samples to differentiate the boundary

CONTACT M. Balsi marco.balsi@uniroma1.it DIET, Università "La Sapienza", via Eudossiana 18 00184, Rome, Italy

within the tree canopy from the one between the tree canopy, which are not easy to obtain without good reference data.

Methods based essentially on maxima of the CHM are very efficient for forests that are composed of trees, such as conifers, that have a well-defined apex, are sufficiently separated from each other, and are sufficiently uniform in height so that most trees are not covered by taller neighbors. Fusion of other information (in particular visible and IR imagery) may improve results due to higher spatial density, while LiDAR-derived CHM guarantees accuracy in height estimation. However, substantial improvement of such techniques is not possible unless the whole point cloud (rather than the highest points only) is exploited. Based on such considerations, several authors have proposed methods that use all the information contained in the cloud, especially using clustering algorithms.

Morsdorf, Meier, Allgöwer, and Nüesch (2003) use k-means clustering directly on a dense point cloud obtained on conifer forests, using local maxima as seeds for the algorithm. A similar approach is taken by Lee, Slatton, Roth, and Cropper (2010). Also Gupta, Weinacker, and Koch (2010), apply k-means on the whole dataset. They show that by scaling the z coordinate (so that the ellipsoidal shape of trees tends to become more spherical) results are improved. They also show that the method works with random seeds, but better results are obtained when local maxima are used instead.

Yao, Krull, Krzystek, and Heurich (2014) use the normalized cuts algorithm to build clusters, adding additional attributes to each point besides XYZ position, such as pulse width and intensity obtained from processing the full-wave response, in order to exploit similarity.

Ayrey et al. (2017) proposed to apply k-means clustering after dividing the point cloud into horizontal layers, looking for consistencies across layers, and starting to form top layers so that local maxima are used as seeds when building 3D clusters form 2D clusters.

Other approaches include an original proposal by V.F. Strîmbu and B.M. Strîmbu (2015), based on iterative building of a graph that hierarchically connects points, and successive visit of the graph for segmentation based on heuristics.

Sačkov et al. (2016) address specifically the problem of dealing with complex forests, in particular broadleaved woodlands and multi-layered canopies. They use the reFLex algorithm, developed by some of the authors, which includes several tree allometry rules on permissible tree heights and crown dimensions in order to increase the likelihood that real trees are detected. Computational efficiency is enhanced by dividing points into three-dimensional regular tiles.

Specifically relevant to the approach taken in this paper is the work of Tittmann, Shafii, Hartsough, and Hamann (2011), who use a modelling strategy searching for simplified tree shapes, by applying the random sample consensus (RANSAC) algorithm with paraboloids directly to the point cloud. As their case study is applied to conifer stands, the paraboloid is indeed a good approximator for tree shapes, and treetops are quite well separated. Also Reitberger, Schnörr, Krzystek, Stilla (2009) use RANSAC, but in this case specifically to find stems (used to identify tree positions), in contexts where canopies are well separated from the ground level.

As pointed out by Sačkov et al. (2016), trees having relatively flat and irregular crowns, and mixed forests containing uneven-aged trees of different species pose a specific challenge to ITD. In this work, we intend to address this kind of problems, starting from a relatively simple case study, yet significant, because we considered a hazel grove, made of trees that have no evident top and several small stems, with the crown extending practically down to ground level. In such context, we propose the use of a methodology based on fitting and modelling the 3D-shape of the tree using RANSAC (Fischler & Bolles, 1981) applied to primary raw data, in order to improve performance both in tree detection and crown reconstruction. Comparison with area-based approaches (ABA – Kaartinen et al., 2012; Sačkov et al., 2016) is also provided.

Data set

The data has been collected by Oben during a project demonstration at Natural Reserve of Lake Vico, Caprarola, Italy (N42.343 E12.163).

The airborne laser scanner (ALS) dataset was collected using YellowScan LiDAR, mounted on a RPAS, with the following technical specifications: 1.8 m-diameter octo-copter, permitting GPS waypoint navigation, auto take-off and landing, a payload up to 4 kg and 20 min cruise-range. In Figure 1 the system during flight is shown.

The Yellowscan LiDAR is integrated with internal INS and GPS receiver enhanced by RTK (Real Time Kinematics). Dimensions, weight and autonomy of this LiDAR are about 17 × 21 × 15 cm^3, 2.1 kg, and 3 h, respectively. Such characteristics make this LiDAR a good solution for light UAV applications. The LiDAR operates up to 100 m above ground level. It provides high-density measurements with accuracy better than 40 cm under the best condition of use. Scan angle range is ±50°. The system provides up to three echoes per shot, allowing also to obtain returns from ground under vegetation cover, exploiting gaps that are present even in dense canopies. In any case, previous analysis of data obtained in similar

Figure 1. Remotely Piloted Aerial System carrying the LiDAR.

conditions using the same scanner showed that the percentage of second and third echoes is very low, less than 5%, and therefore not very much useful to help the classification. For this reason, information on return number was not used in the processing.

The dataset covers an area within a hazel grove of 181 trees. The strip scanned yielded a point density of about 40 points/m^2 (all returns) or equivalently a mean spacing of about 0.16 m. Our data show higher point density than conventional ALS solutions. Ground points were filtered out by means of a classification software (Forlani & Nardinocchi, 2007) and normalized data with respect to the ground were used in the following.

In order to analyze data and results in deep detail, we concentrate on a small area, Figure 2, without loss of generality.

Application on the whole area is considered at the end of this study. The case study considered in this work is simplified with respect to a general one because only one species is present and age is also uniform. Nevertheless, the case is significant because this type of trees is characterized by crowns that have no evident apex at the center, so that methods based on local maxima are not efficient. Therefore we consider it appropriate to develop our method, while application to the general case containing trees with different age and species will be considered in future work.

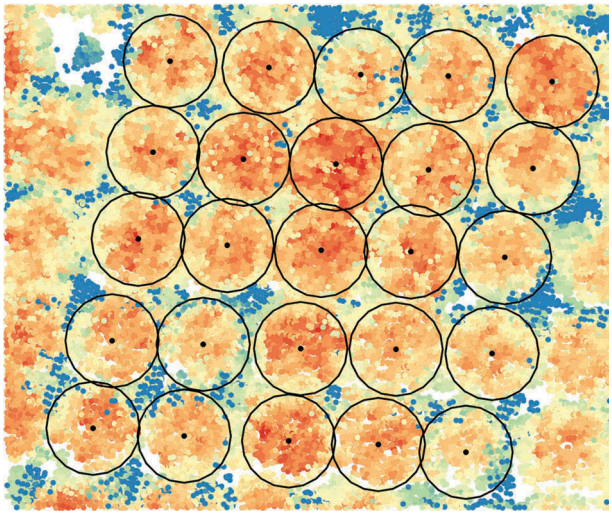

Figure 2. Region of interest considered in the case study. Highest LiDAR return points are colored according to height, normalized to ground level. Black points correspond to true position while black circles indicate conventional extension of individual trees, assumed with a radius equal to a mean value of 2.5 m.

Ground truth was not available in the area under study by on-site survey. However, based on the CHM and on Google Earth orthophotograph, and exploiting the regularity of the plantation, circles were drawn manually by an expert indicating the position of observable trees (Figure 2). Their real extension has not been estimated and a mean value of 2.5 m has been heuristically assigned to the radius of a circle corresponding a tree.

Single-tree detection in high-density LiDAR data

Our algorithm works directly on the point cloud, using all points in the volume scanned, looking for characteristic shapes of trees. It is addressed to trees that have no evident top and that could present several small stems which would mislead methods based on local maxima (LM) and/or exploiting the highest points of the cloud only.

Most points are located near the surface of the crown, that appears relatively empty, and despite the fact that the top is rather flat and irregular, sometimes even showing all local maxima on the edge rather than near the center. As shown in Figure 3, hazel crowns can be roughly approximated by a spherical cap.

The RANSAC algorithm (Roth & Levine, 1993) was set to search for spherical models in the point cloud. Such a shape requires a minimal set of points to instantiate its free parameters. A minimal set is the smallest number of points required to uniquely define a given type of geometric primitive (e.g. four in the case of sphere). After choosing one minimal set at random, the algorithm tests how many points of the point cloud are approximated by this shape within a defined threshold. After a fixed number of such trials,

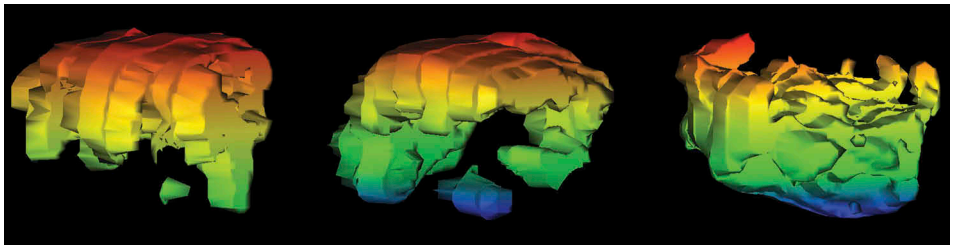

Figure 3. Reconstructed volumes of individual trees. The layered shapes are due to the pattern imposed on points by laser rotation.

the shape which is approximated by the largest number of points is chosen and the algorithm may go on to search another one in the rest of the data. The number of trials or candidates T required to detect the desired shape depends on the probability to detect the correct model and the probability to have outliers in the cloud points (Schnabel, Wahl, & Klein, 2007). RANSAC is a very robust method and it can deal with data with more than 50% of outliers.

In such a large point cloud (even the small volume of our test case, which is orders of magnitude smaller than a practical case, contains about 50,000 points), the set of hypotheses tested would be very large, impacting computation time, and allowing for many highly unlikely solutions to appear because of the large number of outliers in the data. It is important to underline that RANSAC is able to extract all the shapes in the point cloud that are consistent with the parametric model, but we set it in such a way as to consider only the most relevant present in a small area of the data. Therefore, we chose to provide as input to the algorithm the point clouds included in a candidate region of interest (RoI) having small dimension (in this case 4 m×4 m) in order to be mainly consistent with only one tree or a portion of it. Moreover, it should be noted that we do not expect the RoI to completely contain one tree, but rather that it should contain a significant set of points, appropriate to extract the shape of one tree. This partially eases the need to know the dimension of trees, which is in general not uniform. In any case, the issue of appropriate tree scale is an important one (Liu et al., 2015), and we shall deal with it more thoroughly when we address the case of mixed forests in the future.

In this work, we tested two solutions for defining the centers of the RoI's. In the first one, we used the tree candidates resulting from ABA methods application, while in the second one arbitrarily spaced seed points are used. In Figure 4 our data processing workflows are shown.

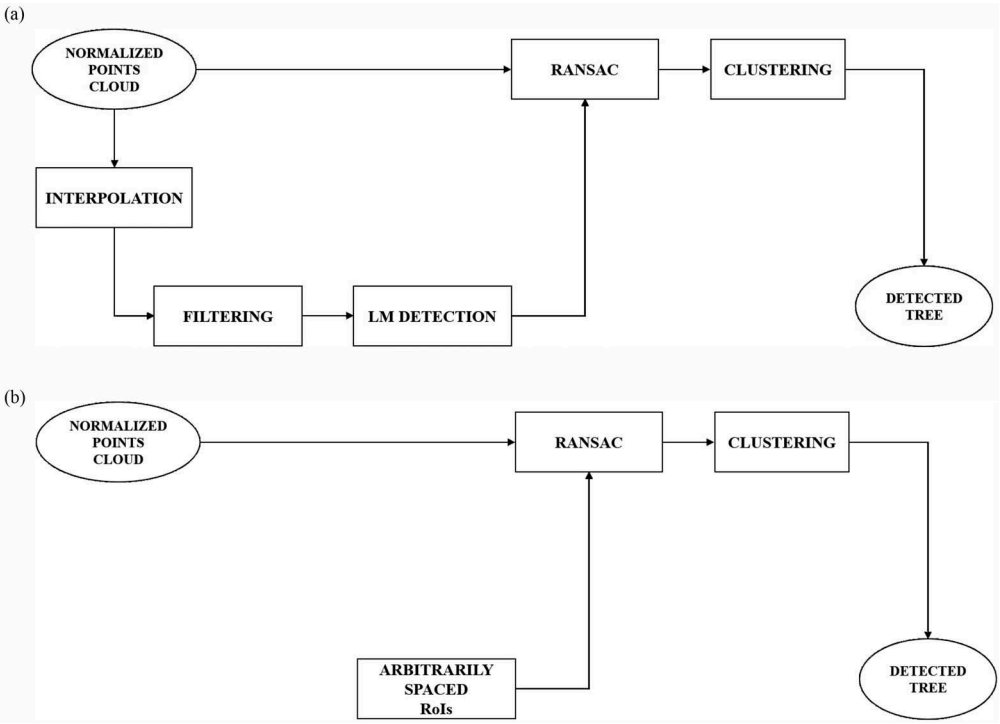

Figure 4. (a) Flow chart of the tree detection algorithm using candidate RoI from ABA – (b) algorithm using arbitrarily-spaced RoI's.

In both cases at the heart of our algorithm is RANSAC. Key parameters include the minimum number of points required to accept a shape candidate, fixed at 300 points (considering that on average 1500 points define a tree and a window slightly smaller than the average crown size has been used). Moreover, considering the scattering of the data, in particular around the crown, a large threshold of 10 cm was chosen to accept points as fitting the model. In our method, RANSAC was set in such a way as to accept only the first detected sphere starting from each RoI. Therefore, if e.g. the RoI includes points from two trees, only the most relevant should be extracted from that RoI.

Even applying RANSAC on RoI's as described above, several spheres could be detected for each tree, because the same tree can be present in several RoI's. In fact, the multi-scale approach (LoG) yields many candidates RoI's, while the LOCM approach is sensitive to presence of several maxima at the edge of the crown. Moreover, in the case of arbitrarily spaced seed points approach, it happens because several seed points fall nearby the tree.

In order to obtain only one center for each tree, a clustering algorithm is added to the workflow to group results of RANSAC according to consistency of positions, based on the fact that several spheres obtained for the same tree have close centers. In this work, we chose the basic *k-means* (Jain, 2010) method, without employing advanced variations of the method. Therefore, we set the number of the clusters equal to the number of the trees defined by the ground truth, and applied Euclidean distance. In the general case, where no a priori knowledge about of the number of the trees is available, other clustering solutions should be used, that include automatic choice of the number of clusters. Although it is out of the scope of this paper to solve such issue, as possible solution in the above-mentioned scenario we mention DBSCAN (density-based spatial clustering of applications with noise) algorithm (Ester, Kriegel, Sander, and Xu (1996).

Concerning the choice of the RoI's, that makes the distinction between the two algorithms we applied, first discuss the case of Figure 4a, where centers of the RoI's are placed in tree candidate positions obtained from ABA methods and then the case where centers of RoI's are placed uniformly spaced across the data (Figure 4b).

RoI from ABA

At the first stage, the raw point cloud is filtered and interpolated over a grid. Such strategy reduces computational burden, but at the same time the data structure used allows to go back, if necessary, to the raw points of each grid cell. A first issue is to define the kind of interpolation used to produce the gridded data. In fact, the point cloud has very high density and several points fall into a single grid cell: the algorithm will choose the highest point if it is higher than a given threshold loosely depending of the kind of trees, otherwise the null value (ground) is assigned to the grid cell. The second issue is to define the size of the grid cell; taking into consideration the density of the point cloud, two different grid sizes, respectively of 25 cm and 50 cm have been used in this work (Figure 5). Obviously, the bigger the size the larger the smoothing of the data.

At the second stage, the interpolated grid is filtered to find local maxima. In this work, we have focused our attention on two algorithms: local maxima finding (LOCM), and LoG, as described by Kaartinen et al. (2012). In particular, the impulse response of the first filter is a 3×3 Laplacian approximation, whereas the impulse response of the second filter has a square window kernel whose size depends on the standard deviation σ of the base Gaussian function. Compared to LOCM, LoG filter shows interesting properties:

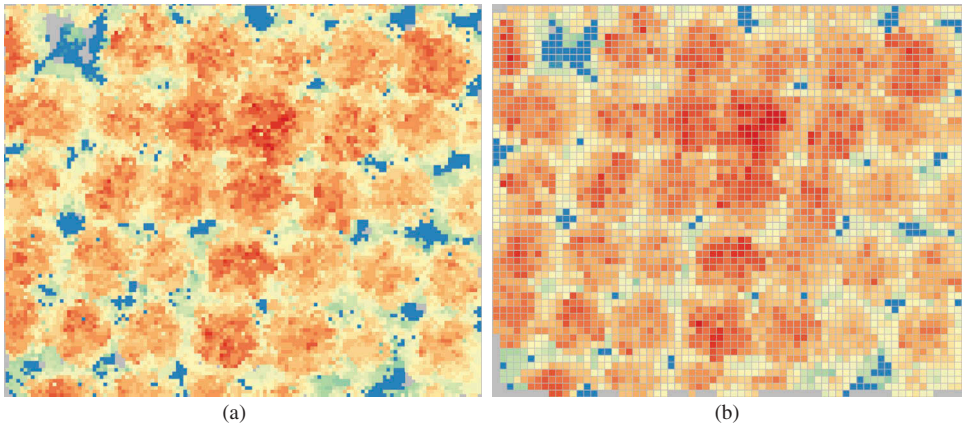

(a) (b)

Figure 5. Gridded data. (a) 25 cm grid size; (b) 50 cm grid size.

- the filter applies the Laplacian operator to a smoothed version of the data;
- filter pass band depends on σ (scale factor);
- scale factor can be chosen to optimize the detection. In fact, by choosing a kernel size that is comparable to the expected tree crown size, it is possible to maximize the number of cases in which a unique maximum for each tree is extracted, as desired.

At third stage, the LM detection is applied. It starts from maximum height LOCM filtered value or from minimum LoG value, respectively. The process of segmentation goes on until no more points having negative gradient can be added to the region. The same process is started from another maximum (or minimum) until all pixels are assigned to a region or are excluded by the process, because close to ground level or belonging to positive value. The output of this stage are tree positions corresponding to the seed points of every region. The tree candidate positions thus obtained are then used as centers for the RoI's used in RANSAC.

The algorithm of Figure 4b is motivated by the fact that the RANSAC algorithm shows good performance even based on LM results that are far from satisfactory.

RoI from arbitrarily spaced seed points

As commented above, in the case study considered, but even more in the case of mixed hardwood forests, methods based on local maxima have rather poor performance. For this reason, we are especially interested in testing performance of the RANSAC-based approach avoiding the use of LM altogether. For this purpose, we chose RANSAC RoI's by placing them over an arbitrary grid of centers, that is made in such a way as to have 50% overlap of the RoI's with neighbors in the four directions, and to have them spaced more than double as close as tree centers, so as to cover all cases of relative spacing with respect to real trees, (black dots in Figure 6).

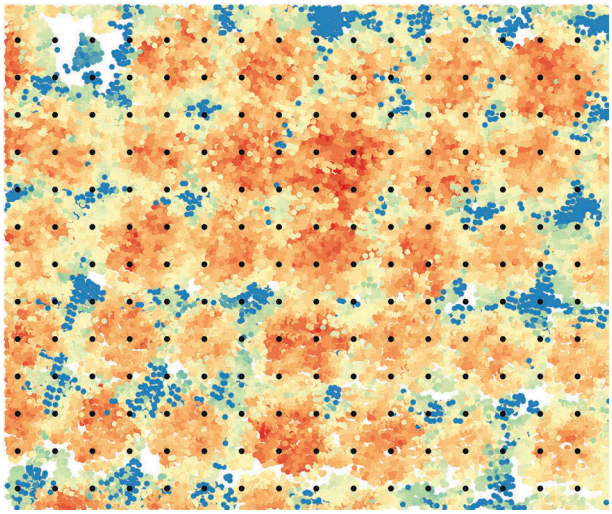

Figure 6. ROI centers (black dots) located on arbitrary grid.

From ABA to ITD

ABA methods look for local maxima in the data. More specifically, the two ABA approaches that have been taken into account, *LOCM* and *LoG*, produce a modified representation of the CHM (Figures 7 and 8). Both filters have been applied to 25 cm and 50 cm grid size.

Being LoG a multiscale operator it is important to determine the scale range used appropriately. In Figure 8 results at different scales for the 50 cm grid size are shown. Similar behavior is obtained at 25 cm grid size. The green/blue colored pixels correspond to negative values of the Laplacian (indicative of tree tops), while yellow/red colors correspond to positive values (concave areas between trees). It is apparent that too small values of σ produce noisy and imprecise results, and too large values cause excessive blurring, and eventually loss of tree detection due to crowns fusion.

The optimal σ value depends on the size of the object to extract (trees) and we observe (Figure 9) that it corresponds to the value that produces the lowest number of negative values, which are 3.0 m for 50 cm grid size and 5.5 m for 25 cm grid size.

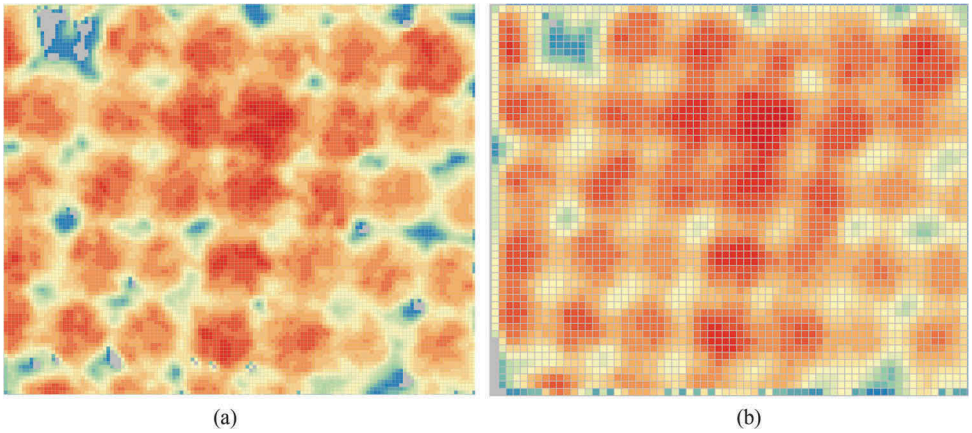

(a) (b)

Figure 7. CHM filtered with LOCM. (a) 25 cm grid size; (b) 50 cm grid size.

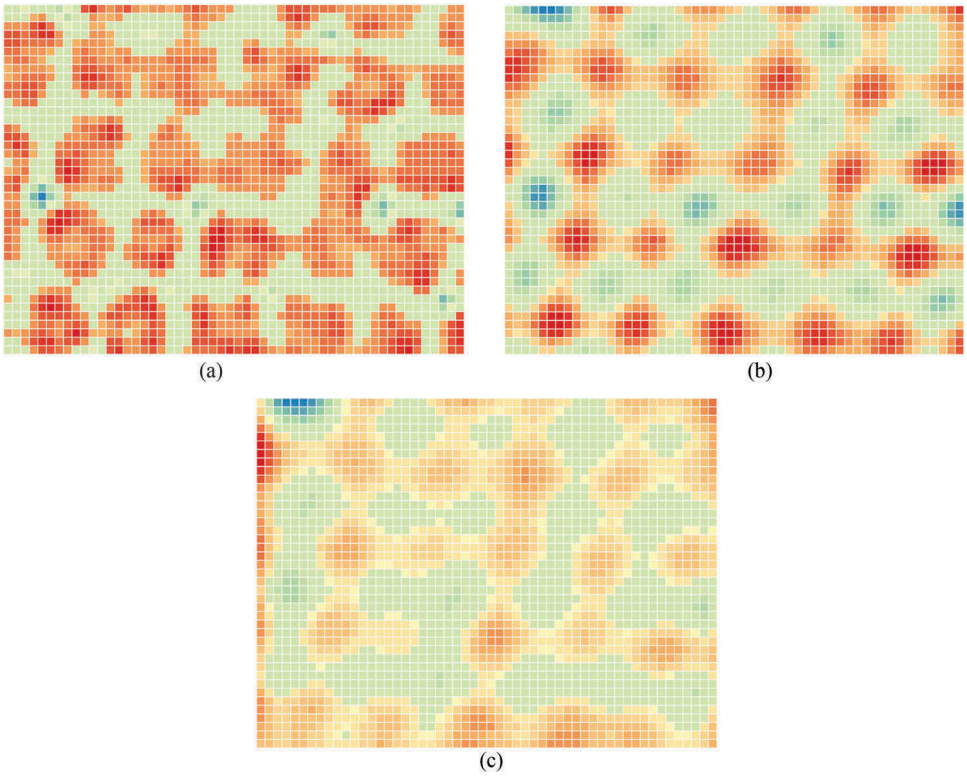

Figure 8. CHM filtered with LoG. (a) σ = 1.5; (b) σ = 3.0 (c) σ = 4.0.

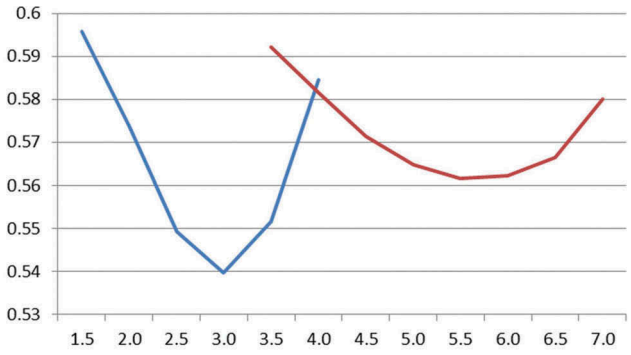

Figure 9. Percentage of negative values in data filtered with LoG at variable scale σ.

Obviously, such optimal scale can be chosen in presence of trees having similar size. In general, it is necessary to apply a multiscale approach, looking for the recurring presence of a tree across several scales. More specifically the range between 2.0 m and 4.0 m for 50 cm grid size has been used, and the range from 4.5 m to 7 m for 25 cm.

LM detection and ABA tree segmentation

Results of the watershed segmentation of LOCM- and LoG-filtered data are shown in the following. Figure 10a shows fragmentation caused in LOCM by the smaller grid size. The rather irregular tree segmentation obtained by LOCM is also apparent in Figure 10. In fact, data are extremely noisy, without an evident local central maximum. Even with 50 cm grid size (Figure 10b), which works better, some crowns get fused and others lost.

Figure 11 shows the result of LoG segmentation at three different spatial scales, highlighting the fragmentation caused by the filter with too-small σ (case a) and the excessive enlargement due to too-large σ (case c). As above said, the segmentation produces clusters corresponding to tree-region hypotheses. The better behavior of LoG filtering compared to LOCM, in terms of regularity and delineation, is evident, caused by more effective filtering of the data.

It is important to highlight that the tree positions obtained from LoG filtering do not correspond to the center of the region but to the position of the highest point of the region. In fact, discrepancies from the

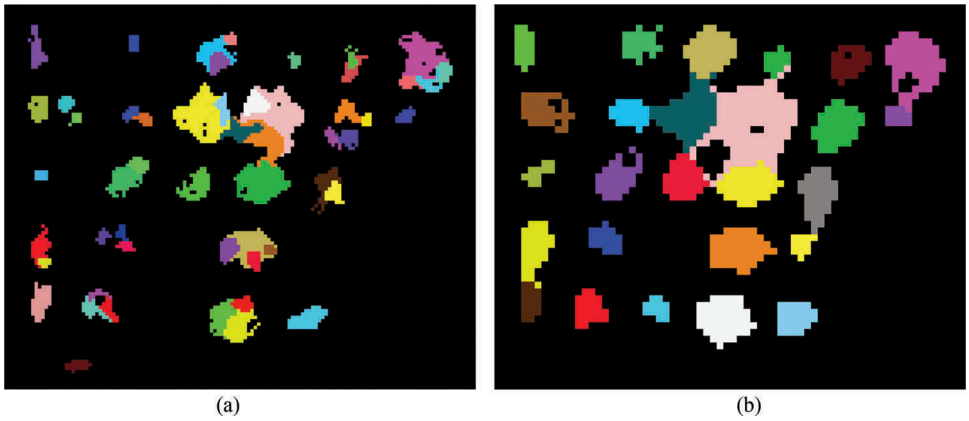

Figure 10. LOCM watershed-based tree segmentation: (a) 25 cm grid size; (b) 50 cm grid size.

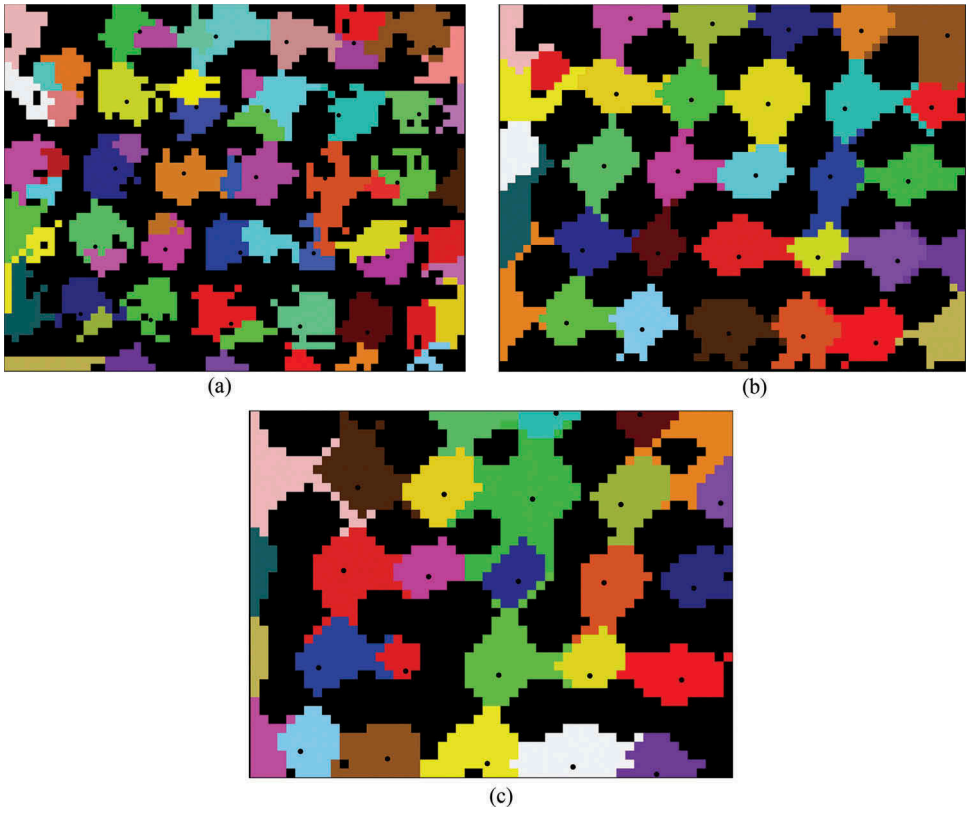

Figure 11. LoG watershed-based tree segmentation (50cm grid): (a) σ = 1.5; (b) σ = 2.5 (c) σ = 4.0. Black dots denote ground truth.

center of the crown (o dispersion of the solutions) as large as 2 m arise, as it is possible to observe in Figure 12, where tree candidates from LOCM and LoG approach are shown. It is to note how the LOCM approach misses several trees: six and four of a total of 25, respectively with 25 cm and 50 cm grid size.

From gridded to raw data

Application of RANSAC on RoI's obtained by ABA produces evident improvement to the tree position detection, and to crown identification. Figure 13 illustrates tree identification using our algorithm as described above (Figure 4a). In this case, tree positions detected are associated to the centers of the spheres chosen by RANSAC, and do not correspond to crown maxima.

Tree positions were displaced up to 2.5 m from those obtained by ABA. The effect of RANSAC is to concentrate the estimated tree positions toward the center of the ground truth area and separating more clearly the regions corresponding to each tree. Results obtained from 25 cm grid size (blue points in Figure 13) present larger dispersion; moreover, while LOCM produces a rather high number of false negatives, on the contrary the LoG approach produces false positives. Finally, the crown delineation (Figure 14) obtained mean value of crown radius respectively at 2.26 m and 2.64 m for 25 cm and

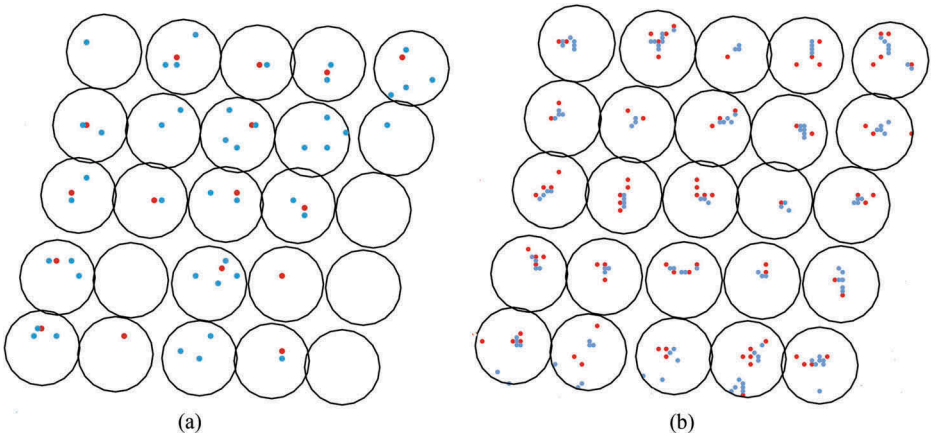

Figure 12. Tree candidates; (a) LOCM results; (b) multiscale LoG results. Candidates obtained with 25 cm grid size are colored in blue, while those obtained with 50 cm grid size are red. Black circles denote the same heuristically-drawn ground truth as shown in Figure 2 and are useful to assess qualitatively the performance of trees detection by the ABA methods.

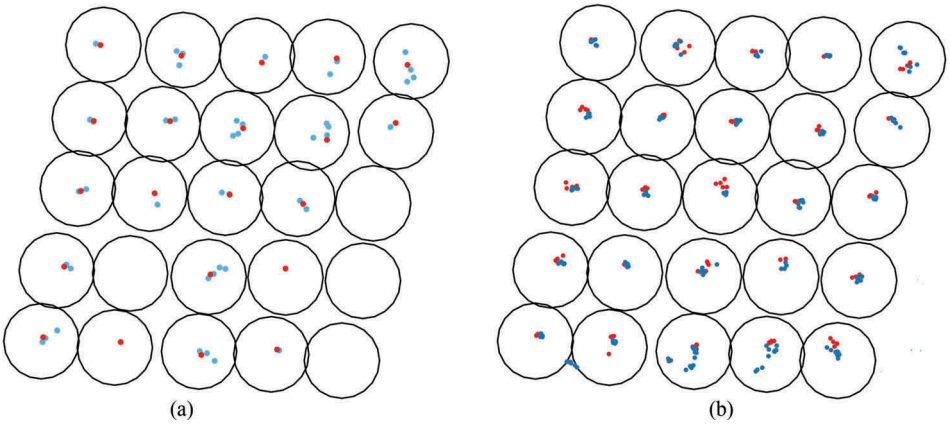

Figure 13. Tree identification after application of RANSAC. (a) using LOCM-based RoI's; (b) using LoG-based RoI's. Candidates obtained with 25 cm grid size are colored in blue, while those obtained with 50 cm grid size are red.

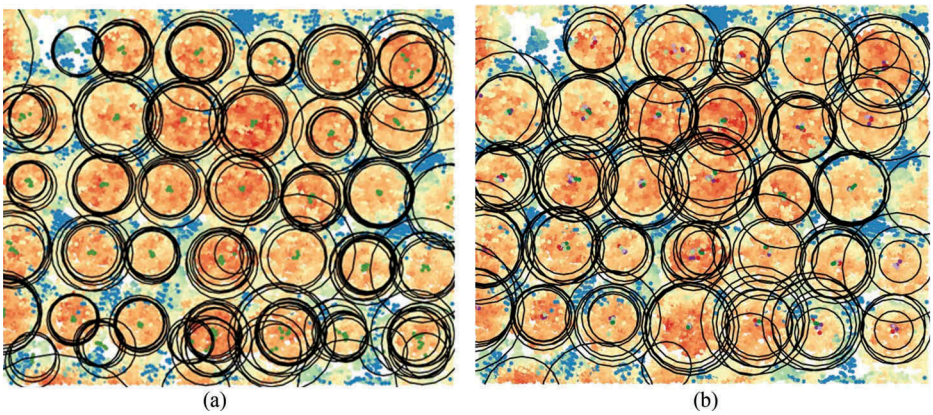

Figure 14. Crown delineation. (a) from 25 cm grid size; (b) from 50 cm grid size. Black circles describe the width of spheres detected by RANSAC. Dots with colors that do not match the region that contains them are centers of RANSAC spheres.

50 cm grid size, both with standard deviation of 0.6 m. In Figure 14, black circles correspond to the width of each detected sphere and should be compared to the ground truth circles of Figure 2. It is apparent that most circles are correctly placed and sized. Some spheres were also detected in wrong position: these correspond to false positives and should be counted as errors of the algorithm. Other spheres are correctly placed with centers closed to the true one, but have excessive diameter, also spanning over neighboring trees. This is a weaker kind of error, that does not affect tree detection per se, but rather

the estimation of its size. Even if we do not have objective data about the true crown size, direct inspection of both LiDAR and visible imaging data allows to determine that the average radius is approximately 2.5 m. Since the RoI's used for both grid sizes have the same dimension (4 m × 4 m) (that means the same raw points were used) we assume that the difference in average sphere radius obtained with the different grid sizes is caused by the random nature of the method (the randomly selected minimum set). In fact, the different runs of the algorithm produce different results, but qualitatively very similar, and average sphere sizes are also highly repeatable.

Finally, it is important to underline that results of RANSAC are filtered according to the assumption that the center of the sphere must lay below the crown of the trees. In fact, a few solutions, which fall between two or more trees, are discarded because the sphere lays above the crown surface.

The false positives extracted on the 25 cm grid size are evident in Figure 14a.

Several trees have been overestimated (15 spheres having radius larger than 3 m out of 215 spheres detected at all scales) when processing the data at 25 cm grid size. At 50 cm grid size 12 outliers (radius larger than 3 m) out of 117 spheres were obtained. It is important to observe that there is no predominant scale that produces such kind of error. The outliers are equally distributed throughout all scales.

The whole area has been processed, which is composed of 181 trees, Figure 15. Processing was performed using only tree candidates produced by LoG approach and a grid size of 50 cm (the combination which presented better performance) was used. Ground truth was extracted from Google Earth: thanks to the regularity of the trees it was possible to obtain quite reliable reference data (Figure 16). The results confirm what was obtained with the test area: no false negatives and several false positives. Moreover, a trend was observed to overestimating the radius of the trees (Figure 15). More specifically, in 19 cases at least one of the spheres obtained for a tree had radius exceeding 3.5 m and was overlapping neighboring trees. However, in all those cases at least one sphere of correct radius was also present.

Clustering

Since RANSAC based on RoI's obtained by ABA produces several hypotheses for crown approximation, though quite consistent among them, in order to define our final choice for tree detection we need to apply further automatization to the process. As observed, centers of RANSAC spheres are quite well clustered, therefore, we expect a clustering algorithm to obtain a good solution easily. To this purpose, we applied a basic k-means algorithm to the spheres centers. Results obtained show that while LOCM-based results are unsatisfactory (because they inherit the poor performance of LOCM – Figure 17), by clustering LoG-based RANSAC results very good estimation of tree position is obtained (Figure 18).

Residual errors are of two types. In some cases a single tree is assigned two clustered centers. By looking at the point cloud directly, and at aerial images, it is possible to see that this typically happens in rather doubtful cases, where the tree shape departs significantly from the expected one or from its expected dimension. In other cases, two trees are fused into one, and the center placed halfway. This case is typically due to the number of clusters chosen (especially where some trees have been split), that constrained

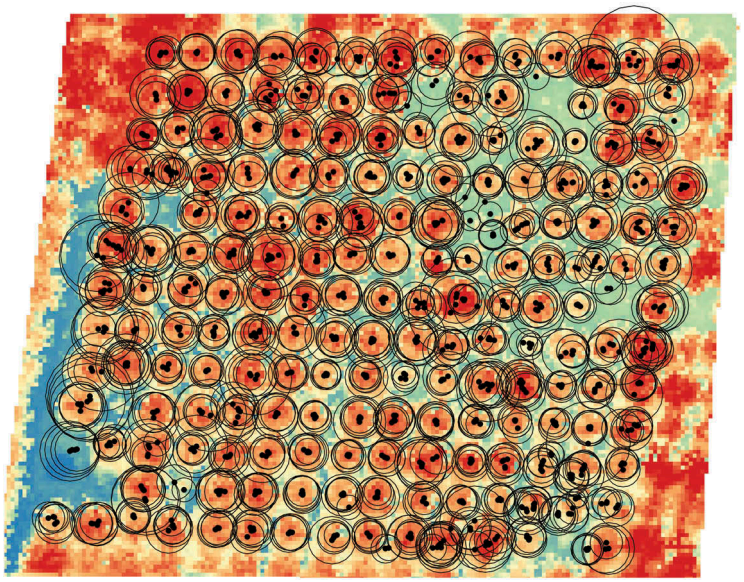

Figure 15. Tree detection and crown delineation of a wider area.

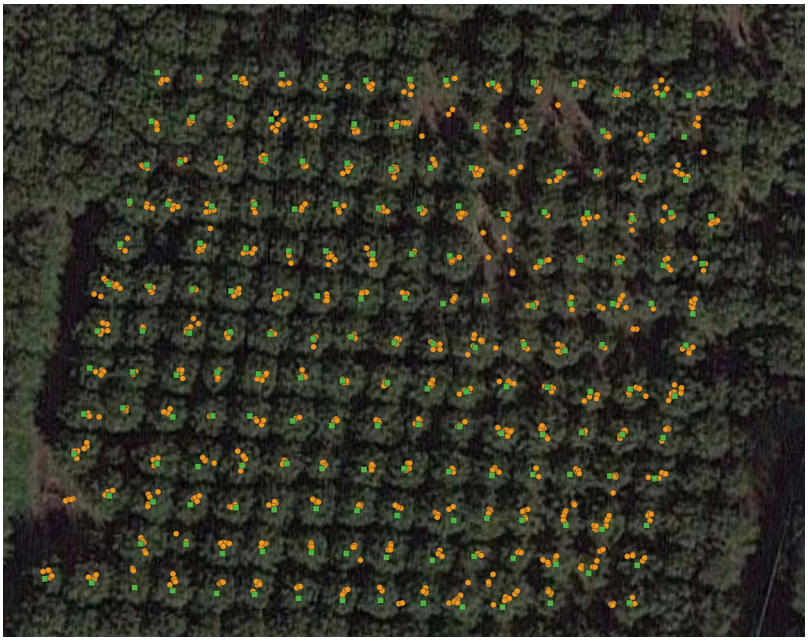

Figure 16. Orthophotograph of the hazel grove considered in this work. Ground truth is represented by green squares denoting tree centers, while orange points represent RANSAC results.

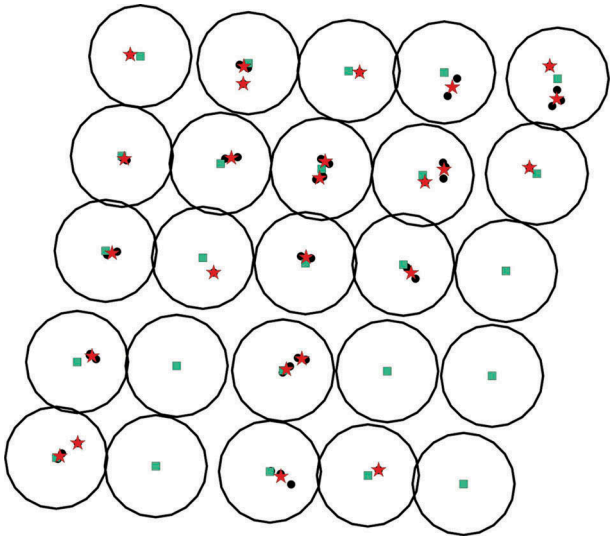

Figure 17. Clustering RANSAC results obtained on LOCM RoI's (25 cm grid). Red stars denote cluster centers, green squares are ground truth circles centers, and black dots RANSAC-detected spheres centers.

the algorithm to fuse the closest clusters elsewhere. In particular, using the 25 cm-grid (Figure 18a), two erroneously split clusters (lower right) caused two couples of well-defined clusters to get fused. With the 50 cm-grid (Figure 18b), one erroneously split cluster (upper center) caused one couple of well-defined clusters to get fused (center-right).

Similar results were obtained on the larger data set. In particular, we can observe that in several cases, there is not a one-to-one relationship between the ground truth and the center of the clusters. It is well known that such problems are typical of k-means as well as of other clustering algorithms, basically because the clustering problem itself is ill-posed (Jain, 2010). As above-stated, more efficient clustering algorithms could be applied, but this is beyond the scope of this paper. In any case, evidence of the errors described can be obtained automatically by measuring intra- and inter-cluster distances. In fact, split clusters maybe spaced at unrealistically small distance, and fused clusters show excessive intra-class average distance, so that automatic splitting might be triggered.

In order to evaluate detection performance, a relationship between ground truth and the cluster centers was established using Euclidean distance. Centers which showed a distance less than a specific threshold (2.5 m) have been labeled as valid trees. In Figure 19 the detection performances are shown. In particular we can observe that 86% of the trees have been detected and 14% missed. We also obtained 11 erroneous tree detection (false alarms).

Working without LM

As commented above, in the case study considered, but even more in the case of mixed hardwood forests, methods based on local maxima have rather poor performance. For this reason, we are especially interested in testing performance of the RANSAC-based approach avoiding the use of LM altogether. For this purpose, we chose RANSAC RoI's by placing them over an arbitrary grid of centers, that is made in such a way as to have 50% overlap of the RoI's with neighbors in the four directions, and to have them spaced more than double as close as tree centers, so

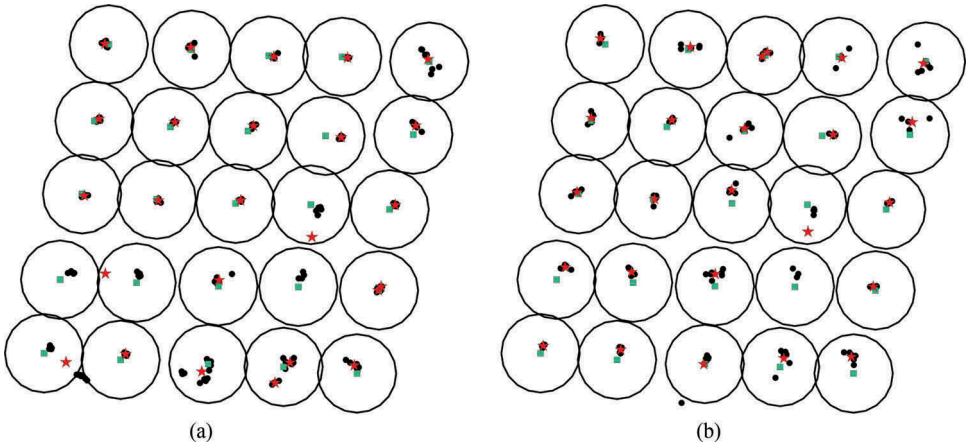

Figure 18. Clustering RANSAC results obtained on LOG RoI's: (a) 25 cm-grid; (b) 50 cm-grid. Symbols as in Figure 17.

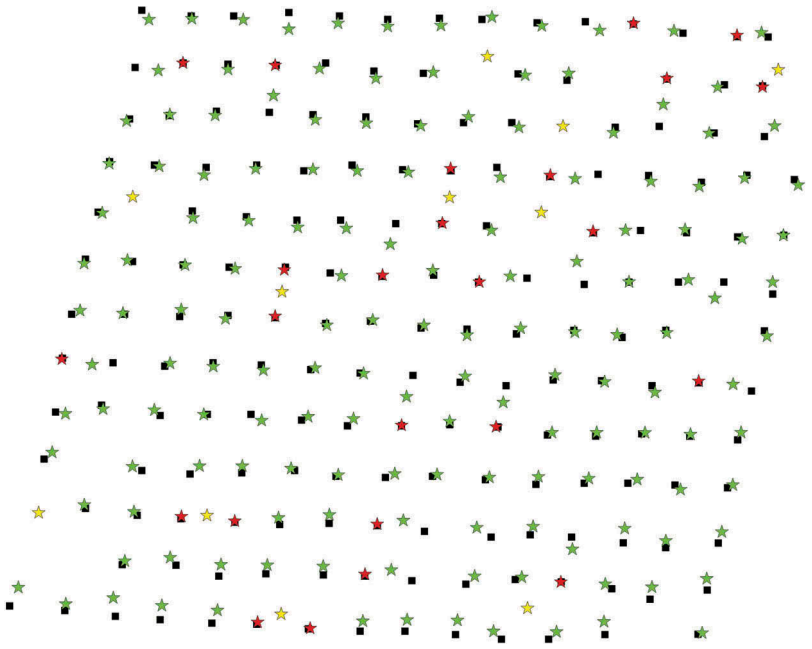

Figure 19. Detection performance on the whole data set. Black squares indicate ground truth, green stars are correctly placed cluster centers, red stars are missed detection, yellow stars are false alarms.

as to cover all cases of relative spacing with respect to real trees, Figure 20. Results obtained in this case (Figures 20 and 21) are not as good as when using LOG-based RoI's, but is quite encouraging to see that performance is only slightly degraded, so that operation totally based on the raw point cloud appears indeed feasible.

As expected, RANSAC algorithm does not find any shape model for several points (starting from 238 seed points only 78 trees have been found), but the solutions are not as well grouped as in the ABA-based case. Obviously, such dispersion in the tree candidate positions causes more uncertainty in tree extension. Deeper analysis has to be conducted starting from these preliminary results. It is important to highlight that at the present state of the art, a refinement by least square adjustment of the chosen consensus set has not been performed.

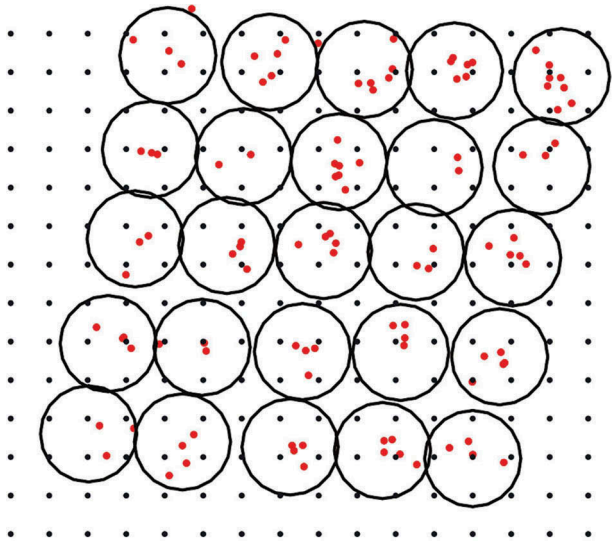

Figure 20. RANSAC results obtained on arbitrary spaced grid. Red dots denote RANSAC-detected spheres centers, and black dots define our arbitrarily-spaced grid. Grid spacing is 2 m.

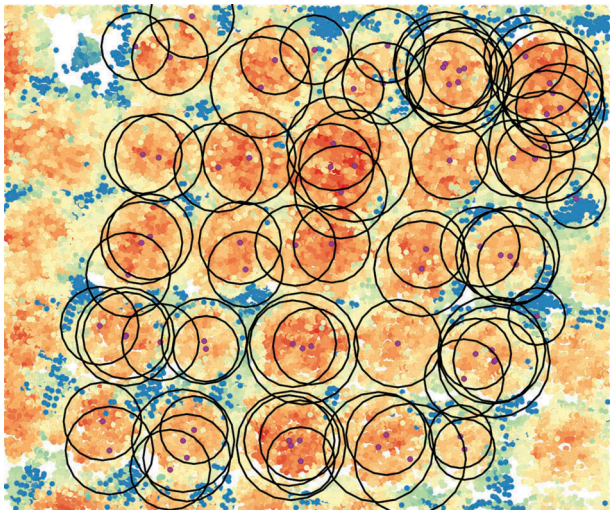

Figure 21. Tree extension of the detected trees (RANSAC with arbitrarily-spaced RoI centers).

Figure 22 shows clustering results of the result with arbitrarily-spaced RoI centers. Even if in this case RANSAC results are not as good as those obtained with LoG-based RoI's, the k-means algorithm classified every tree correctly (i.e. all trees were detected).

Conclusions and perspectives

The RANSAC algorithm has been applied to ALS point clouds obtained over a hazel grove, that is characterized by trees that have no evident apex, with irregularly-shaped crown extending close to ground. This case is simpler than the mixed hardwood forest case, that is the final purpose of our work, but poses a basic challenge that ABA methods, quite efficient on favorably-shaped trees (e.g. conifer forests) cannot solve satisfactorily.

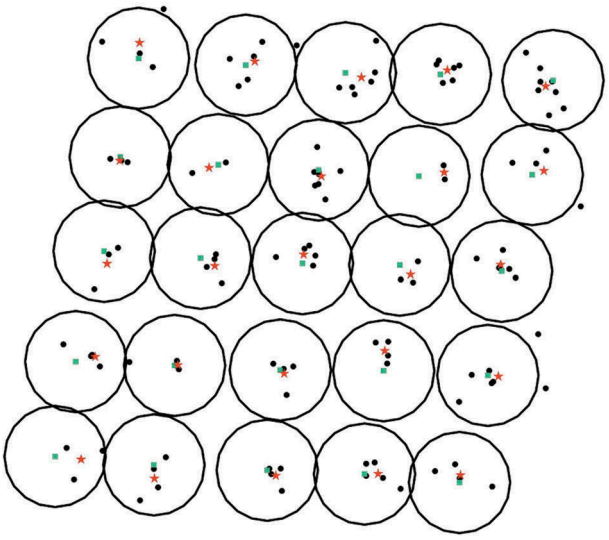

Figure 22. Clustering RANSAC results for the arbitrarily-spaced RoI algorithm. Red stars denote cluster centers, green squares are ground truth circles centers, and black dots RANSAC-detected spheres centers. As in other figures, black circles denote heuristically-drawn ground truth and are meant useful to assess qualitatively the performance of trees detection. In this case, every cluster is associated to one and only one tree.

Results show that RANSAC (followed by k-means clustering) improves detection of tree crown with respect to ABA results, and that even when no information on local maxima is used, ITD can be considerably improved.

Deeper analysis of some issues concerning application or the RANSAC algorithm appears necessary, first of all the application of a final least square adjustment to the consensus set found. Continuation of the work will build on the experience obtained to address more difficult cases.

In the case of mixed forests, trees have different shapes and heights, and many of them are hidden under or between taller and larger ones. Application of the RANSAC algorithm in such environment will involve adding one more free parameter to deal with ellipsoidal shapes, with one vertical axis. Integration of the methods proposed with layered approaches (e.g. Ayrey et al., 2017) appears as a promising option, as well as exploitation of coordinated data, such as visible and IR imaging. Such additional techniques will be used both to improve initial guesses over the completely random, or regular-grid-based approach, and to select the most likely candidates emerging from RANSAC prior, or instead of, clustering.

Geolocation information

Case study data were acquired near N42.343 E12.163 (Lago di Vico, VT, Italy)

Acknowledgments

Data acquisition was performed during a demo for project FreshLIFE (LIFE14 ENV_IT_000414) funded by the European Union LIFE program.

Disclosure statement

No potential conflict of interest was reported by the authors.

Funding

This work was supported by the European Union LIFE program.

ORCID

M. Balsi http://orcid.org/0000-0002-3571-2353
C. Nardinocchi http://orcid.org/0000-0003-2644-4569

References

Ayrey, E., Fraver, S., Kershaw, J.A., Kenefic, L.S., Hayes, D., Weiskittel, A.R., & Roth, B.E. (2017). Layer stacking: A novel algorithm for individual forest tree segmentation from LiDAR point clouds. *Canadian Journal of Remote Sensing*, *43*(1), 16–27. 07038992.2017.1252907.

Ester, M., Kriegel, H.P., Sander, J., & Xu, X. (1996), A density-based algorithm for discovering clusters in large spatial databases with noise. Proc. of Second International Conference on Knowledge Discovery and Data Mining (KDD'96), August 2-4, 1996 Portland, Oregon, 226–231.

Fischler, M.A., & Bolles, R.C. (1981). Random sample consensus: A paradigm for model fitting with applications to image analysis and automated cartography. *Communications of the ACM*, *24*(6), 381–395.

Forlani, G., & Nardinocchi, C. (2007). Adaptive filtering of aerial laser scanning data. In P. Rönnholm, H. Hyyppä, & J. Hyyppä (Eds.) *ISPRS Workshop on Laser Scanning 2007 and SilviLaser 2007 in Espoo*. Finland. (2007, September 12– 14).

Gupta, S., Weinacker, H., & Koch, B. (2010). Comparative analysis of clustering-based approaches for 3-D single tree detection using airborne fullwave LiDAR data. *Remote Sensing*, *2*, 968–989.

Jain, A.K. (2010). Data clustering: 50 years beyond K-means. *Pattern Recognition Letters*, *31*, 651–666.

Jakubowski, M.K., Li, W., Guo, Q., & Kelly, M. (2013). Delineating individual trees from LiDAR data: A comparison of vector- and raster-based segmentation approaches. *Remote Sensing*, *5*, 4163–4186.

Kaartinen, H., & Hyyppä, J. (2008). *Tree extraction*. European Spatial Data Research, official publication n. 53. Amsterdam: EuroSDR.

Kaartinen, H., Hyyppä, J., Yu, X., Vastaranta, M., Hyyppä, H., Kukko, A., … Wu, J.-C. (2012). An international comparison of individual tree detection and extraction using airborne laser scanning. *Remote Sensing*, *4*, 950–974.

Lee, H., Slatton, K.C., Roth, B.E., & Cropper, W.P. (2010). Adaptive clustering of airborne LiDAR data to segment individual tree crowns in managed pine forests. *International Journal of Remote Sensing*, *31*(1), 117–139.

Li, W., Guo, Q., Jakubowski, M., & Kelly, M. (2012). A new method for segmenting individual trees from the lidar point cloud. *Photogramm Engineering Remote Sensing*, *78*, 75–84.

Liu, T., Im, J., & Quackenbush, L.J. (2015). A novel transferable individual tree crown delineation model based on fishing net dragging and boundary classification. *ISPRS Journal of Photogrammetry and Remote Sensing*, *110*, 34–47.

Morsdorf, F., Meier, E., Allgöwer, B., & Nüesch, D. (2003). Clustering in airborne laser scanning raw data for segmentation of single trees. *International Archives of the Photogrammetry, Remote Sensing and Spatial Information Sciences*, *34*(3), W13.

Reitberger, J., Schnörr, C., Krzystek, P., & Stilla, U. (2009). 3D segmentation of single trees exploiting full waveform LIDAR data. *ISPRS Journal of Photogrammetry and Remote Sensing*, *64*(6), 561–574.

Roth, G., & Levine, M.D. (1993). Extracting geometric primitives. *CVGIP: Image Understanding*, *58*(1), 1–22.

Sačkov, I., Bucha, T., Santopuoli, G., Lasserre, B., & Marchetti, M. (2016). Forest inventory attribute prediction using lightweight aerial scanner data in a selected type of multilayered deciduous forest. *Forests*, *7*(12), 307.

Schnabel, R., Wahl, R., & Klein, R. (2007). Efficient RANSAC for point-cloud shape detection. *Computer Graphics Forum*, *26*(2), 214–226.

Strîmbu, V.F., & Strîmbu, B.M. (2015). A graph-based segmentation algorithm for tree crown extraction using airborne LiDAR data. *ISPRS Journal of Photogrammetry and Remote Sensing*, *104*, 30–43.

Tittmann, P., Shafii, S., Hartsough, B., & Hamann, B. (2011), Tree detection and delineation from LiDAR point clouds using RANSAC. SilviLaser 2011, 2011, October 16–19 – Hobart, AU

Yao, W., Krull, J., Krzystek, P., & Heurich, M. (2014). Sensitivity analysis of 3D individual tree detection from lidar point clouds of temperate. *Forests, Forests*, *5*, 1122–1142.